

Electronic Supplementary Information (ESI)

Design of Fe/Ni-doped N/S-rich carbon with advanced bifunctional electrocatalysis for Zn-air battery

Puxin Weng,^{ab,+} Yaqing Guo,^{c,+} Kun Wu,^{ab} Xin Wang,^{ab} Guo-Quan Huang,^{ab} Hang Lei,^a Yifei Yuan,^{*c} Weigang Lu,^{*ab} Dan Li^{*ab}

^a P. Weng, K. Wu, X. Wang, G.-Q. Huang, H. Lei, Prof. W. Lu, Prof. D. Li

College of Chemistry and Materials Science, Jinan University, Guangzhou 510632, P. R. China.

E-mail: weiganglu@jnu.edu.cn; danli@jnu.edu.cn

^b P. Weng, K. Wu, X. Wang, G.-Q. Huang, Prof. W. Lu, Prof. D. Li

Guangdong Provincial Key Laboratory of Functional Supramolecular Coordination Materials and

Applications, Jinan University, Guangzhou 510632, P. R. China. E-mail: weiganglu@jnu.edu.cn;

danli@jnu.edu.cn

^c Y. Guo, Prof. Y. Yuan

College of Chemistry and Materials Engineering, Wenzhou University, Wenzhou 325035, P. R.

China. Email: yifeiyuan@wzu.edu.cn

Supplementary Experimental Section:

1. Materials and methods

1.1 Materials

All reagents and solvents were purchased from commercial sources and used without further purification. Sugar aldehyde, dithiooxamide, ferric nitrate nonahydrate ($\text{Fe}(\text{NO}_3)_3 \cdot 9\text{H}_2\text{O}$), triethylamine, nickel acetate ($\text{Ni}(\text{CH}_3\text{COO})_2 \cdot 4\text{H}_2\text{O}$), potassium permanganate (KMnO_4), deuterated hydrochloric acid ($\text{DCl}/\text{D}_2\text{O}$), chloroform, CDCl_3 , dimethyl sulfoxide- d_6 ($\text{DMSO}-d_6$), 20% Pt/C, and toluene were purchased from Anhui Zesheng Technology Co., Ltd. Anhydrous DMF, pyridine, sodium bicarbonate (NaHCO_3), methanol, ethanol, ether, dichloromethane, *o*-dichlorobenzene, acetic acid were provided by Sinopharm Chemical Reagent Co., Ltd. Sodium bisulfite (NaHSO_3), 2,4,6-trihydroxybenzene-1,3,5-tricarbaldehyde (Tp), sulfoxide chloride (SOCl_2), hydrazine hydrate, dioxane, hydrochloric acid was used as supplied by Sigma–Aldrich. Anhydrous ethanol was purchased from Shanghai Aladdin Biochemical Technology Co., Ltd. Nafion PFSA Polymer dispersions D520 (5.0 wt%) were provided by Bide Pharmatech Co., Ltd. Materials assembled home-made zinc-air batteries (ZABs) were supplied by Changzhou Utec New Energy Technology Co., Ltd. Deionized water was purified by a Milli-Q system (Millipore).

1.2 Characterization of materials and devices

Powder X-ray diffraction (PXRD) data were collected on Rigaku Ultima IV diffractometer (40 kV, 40 mA, Cu $K\alpha$, $\lambda = 1.5418 \text{ \AA}$) from 1.5° to 50.0° with a step of 0.02° at a scan speed of $3.0^\circ \text{ min}^{-1}$. Thermogravimetric (TG) analyses were performed under the N_2 atmosphere with the temperature increasing rate of $10.0^\circ \text{ C min}^{-1}$ on TA-Q50. Fourier transform infrared (FT-IR) spectra were conducted on Thermo Scientific FT-IR Nicolet iS10 spectrophotometer in the range of $4000\text{--}400 \text{ cm}^{-1}$. N_2 adsorption/desorption measurements were performed on Micromeritics ASAP 2020 Plus

adsorption instrument at 77 K, the samples were activated at 393 K in the vacuum for 24 h before performing. ^1H NMR and ^{13}C NMR spectra were recorded on a Bruker AVANCE III HD 400 spectrometer. SSNMR experiments were carried out on the 14.1T Advance Neo Bruker NMR spectrometers. X-ray photoelectron spectrum (XPS) analyses were obtained by using a Thermo ESCALAB 250XI spectrometer with an Mg K α achromatic X-ray source. Inductively Coupled Plasma Atomic Emission Spectrometry (Agilent 725 ICP-AES) was used to collect the contents of Ni and Fe. AFM images were acquired in tapping mode in the air using a Digital Instrument Dimension 3100. The morphology characterizations and elemental mappings of the samples were investigated by a focused ion beam electron beam microscope (FEI Helios Nanolab G3 CX) and a transmission electron microscope (JEM2100F). The measurement of electrical conductivity was carried out by ST2742B automatic powder resistivity tester.

1.3 Electrochemical measurements

All electrochemical measurements were performed by a CHI 660E electrochemical analyzer with a standard three-electrode system. Typically, a rotating disk electrode (RDE), a graphite rod, and an Ag/AgCl (saturated KCl) electrode were utilized as working electrode, counter electrode, and reference electrode, respectively. For measurements in working electrode, 3.0 mg catalyst was ultrasonically dispersed in the mixture of 0.90 mL ethanol and 0.10 mL Nafion solution to prepare the catalyst ink. Afterward, 20 μL the catalyst ink was slowly loaded on a glassy carbon electrode with about 0.15 mg cm^{-2} mass loading. The cyclic voltammetry (CV) tests were conducted in O_2 and N_2 saturated 0.1 M KOH electrolyte with a scan rate of 50 mV s^{-1} . The ORR/OER activities of the catalysts were tested *via* the RDE in O_2 saturated 0.1 M KOH or 6 M KOH electrolyte at 1600 rpm with a scan rate of 5 mV s^{-1} . Especially, the LSV of the catalyst was measured by

rotating ring-disk electrodes at different rotation speeds from 100 to 2500 rpm with a scan rate of 5 mV s⁻¹. The sweeping potential ranges of ORR and OER were -0.2~1.0 and 1.0~1.8 V, respectively.

The electron transfer numbers (*n*) of ORR were obtained by Koutecky-Levich equation:

$$\frac{1}{J} = \frac{1}{J_L} + \frac{1}{J_K} = \frac{1}{B\omega^{1/2}} + \frac{1}{J_K}$$

$$B = 0.62 n F C_0 D_0^{2/3} \nu^{-1/6}$$

Where *J*, *J_k*, and *J_L* represent the experimentally measured current density, the kinetic limiting current density, and the diffusion-limiting current density, respectively. *F* is the Faraday constant with a value of 96500 C mol⁻¹, *C₀* refers to the O₂ bulk concentration, *D₀* is the diffusion coefficient of O₂ in the bulk solution, *ν* refers to the kinematic viscosity (0.01 cm² s⁻¹), and *ω* is the angular velocity of ring disk. In 0.1 M KOH solution: *C₀* = 1.2 × 10⁻³ mol L⁻¹, *D₀* = 1.9 × 10⁻⁵ cm² s⁻¹.

1.4 Assembly and Test of ZABs

Homemade rechargeable ZABs were assembled for electrochemical measurements. The ZABs were composed of Zn foil as the anode, 6 M KOH solution with 0.2 M Zn(Ac)₂·2H₂O as the electrolyte, and nickel foam loaded with the catalyst as the air cathode. The performance of ZABs was measured by a CHI 660E electrochemical analyzer. Especially, rate performances of ZABs were recorded on the LAND CT2001A test system. For the preparation of the air cathode, 5.0 mg of catalyst was ultrasonically dispersed at least 30 min in 950 μL ethanol and 50 μL Nafion solution. The obtained slurry was slowly dropped on a nickel foam of 2 × 2 cm dimension. LSV curves were measured with a sweep rate of 10 mV s⁻¹. The charge-discharge cycle stability was performed under the current density of 5 mA cm⁻² with a cycle period of 16 min (8 min for charging and 8 min for discharging). The power densities were calculated from charging

polarization curves by the following equation:

$$\text{Power density} = \text{current density} \times \text{voltage}$$

The specific capacities were calculated from the galvanostatic (20 mA cm^{-2}) discharge curves by the following equation:

$$\text{Specific capacity} = (\text{current} \times \text{test hours}) / (\text{consumed Zn plate mass})$$

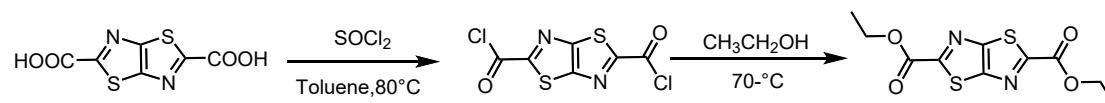
2. Experimental Section

2.1 Synthesis of 2,5-thiazolo[5,4-*d*]thiazole-5-carboxylic acid

2,5-thiazolo[5,4-*d*]thiazole-5-carboxylic acid was synthesized according to previously reported literature.¹⁻² Typically, sugar aldehyde (1681.9 mg, 17.5 mmol) and dithiooxamide (877.5 mg, 7.3 mmol) were dissolved in 40 mL of anhydrous DMF and stirred at 140 °C under an N₂ atmosphere for 12 h. After cooling to room temperature, distilled water (50 mL) was added to precipitate the crude product and washed with ethanol and ether. The crude product was dissolved in the hot chloroform to obtain filtrate and treated with rotary evaporation, then dried to obtain the brown product (1180.6 mg, 59%). ¹H (400 MHz, CDCl₃, ppm): δ = 6.60 (*dd*, *J* = 3.2 Hz, *J* = 1.6 Hz, 2H); 7.10 (*d*, *J* = 3.2 Hz, 2H); δ = 7.58 (*d*, *J* = 1.6 Hz, 2H).

The above product (300.0 mg, 1.1 mmol) was dispersed in 8.38 mL pyridine and stirred at 130 °C for 10 min, cooled to 70 °C, and then 2.14 mL distilled water was added into suspension, cooled to room temperature, and potassium permanganate (1.83 g, 11.6 mmol) was slowly added, then 2.10 mL water was added and stirred at 50 °C for 12 h. Next, sodium bisulfite (170.0 mg, 1.6 mmol) and 2.80 mL of water were added into the mixture to remove unreacted potassium permanganate, then the mixture was filtered to collect filter solution, while the brown cake-like substance formed solid was dispersed in 30.0 mL water at 80 °C for 2 h and filtered again it to obtain the filtrate, the above process was again operated twice. The collected filtrate solution was acidized with concentrated hydrochloric acid to obtain precipitate, and washed with water, dioxane, and ether. The precipitate was vacuum-dried at 100 °C for 24 h to afford 2,5-thiazolo[5,4-*d*]thiazole-5-carboxylic acid (100.7 mg, 40%). ¹³C (100 MHz, DMSO-*d*₆, ppm): δ = 153.95; 161.06; 163.85.

2.2 Synthesis of 2,5-thiazolo[5,4-*d*]thiazoledicarboxylic acetate



2,5-thiazolo[5,4-*d*]thiazoledicarboxylic acid (0.30 g, 1.30 mmol) and excess sulfoxide chloride (4.5 mL) were dissolved in toluene with a drop of DMF solvent as the catalyst and stirred at 80°C for 4 h. Then, the solvent and excess sulfoxide chloride in the mixture were removed by rotary evaporation, and anhydrous ethanol (15 mL) was quickly added into the mixture and reacted at 70°C for 8 h. After the solvent was removed by rotary evaporation, the crude product was dissolved in dichloromethane and mixed with a saturated NaHCO_3 aqueous solution. The organic phase was obtained by extraction, and the organic solvent was removed by rotary evaporation. The obtained precipitate was vacuum-dried at 100°C for 12 h to give the product (339.3 mg, 91%). The ^1H NMR, ^{13}C NMR of 2,5-thiazolo[5,4-*d*]thiazoledicarboxylic acetate are depicted in Fig. S1. ^1H (400 MHz, $\text{DMSO-}d_6$, ppm): $\delta = 4.47$ (*dd*, $J = 14.4$ Hz, $J = 7.2$ Hz, 2H); $\delta 1.37$ (*t*, $J = 7.2$ Hz, 3H). ^{13}C (100 MHz, $\text{DMSO-}d_6$, ppm): $\delta = 14.54$; 63.57; 154.00; 159.57; 162.30.

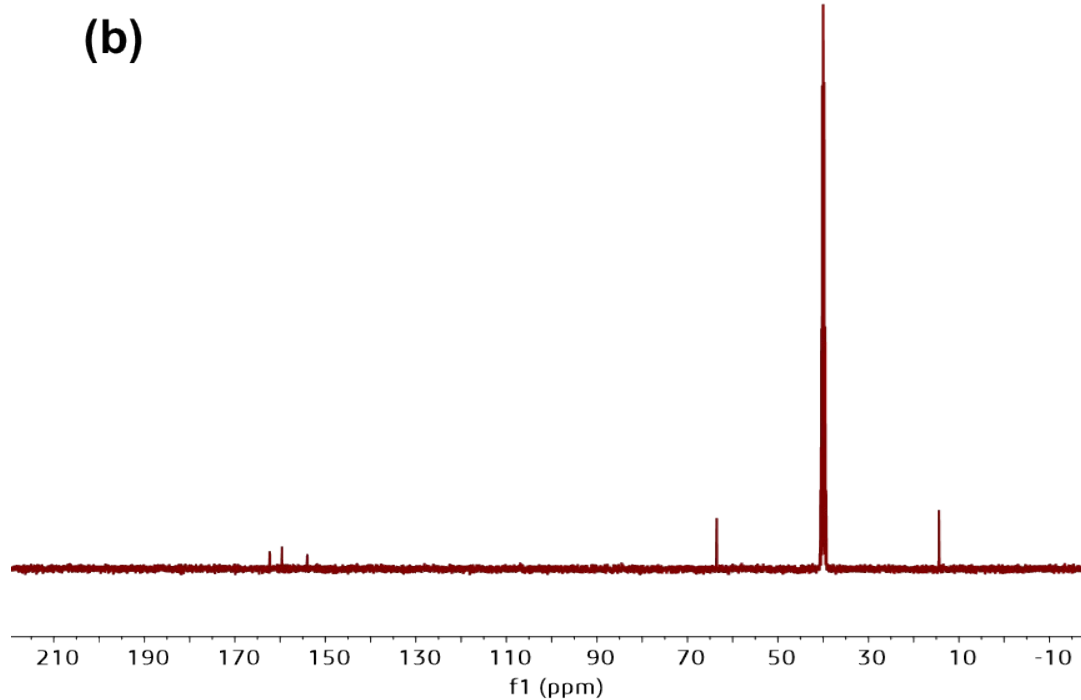
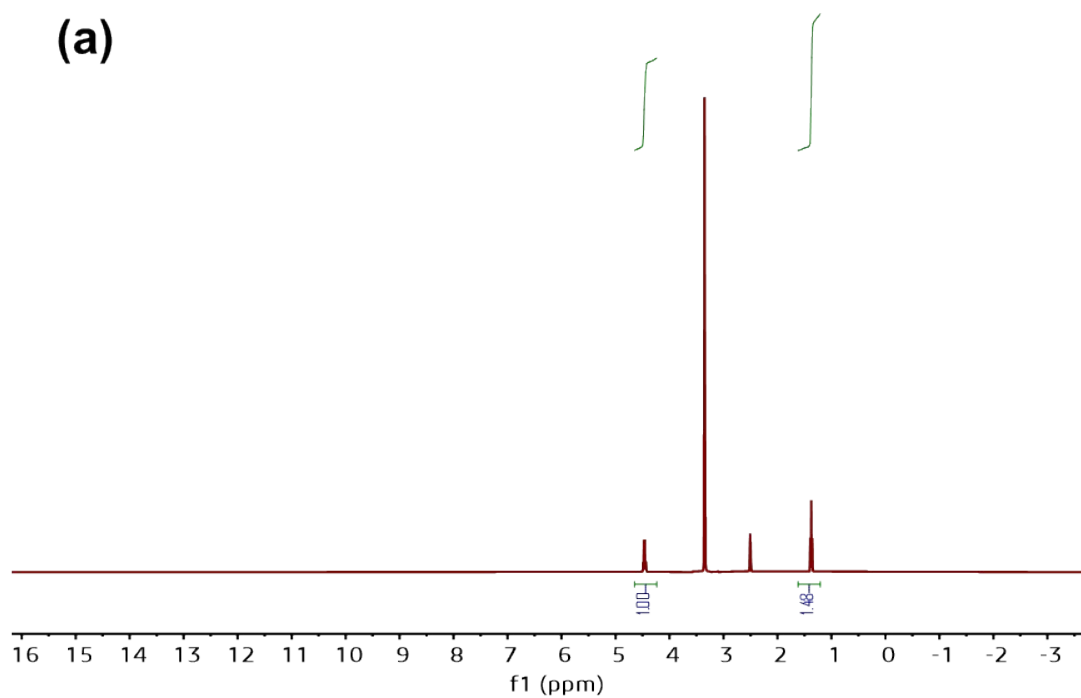
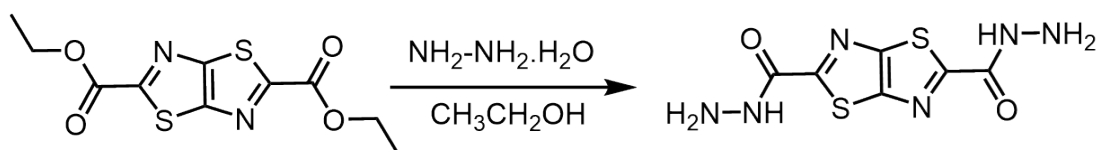


Fig. S1. (a) ^1H NMR spectra of 2,5-thiazolo[5,4-*d*]thiazolidedicarboxylic acetate. (b) ^{13}C NMR spectra of 2,5-thiazolo[5,4-*d*]thiazolidedicarboxylic acetate.

2.3 Synthesis of 2,5-thiazolo[5,4-*d*]thiazolidedicarboxylic hydrazide (Tz)



The above product (0.50 g) was dissolved in 20 mL of ethanol under ultrasonic treatment, then the

solution was added with 3.0 mL of hydrazine hydrate and stirred at 70 °C for 12 h, and washed the precipitate with ethanol and methanol, and vacuum-dried to obtain a light-yellow product (387.6 mg, 86%). The ^{13}C NMR of Tz is depicted in Fig. S2. ^{13}C (100 MHz, $\text{DMSO-}d_6$, ppm): $\delta = 153.64$; 158.39; 163.89.

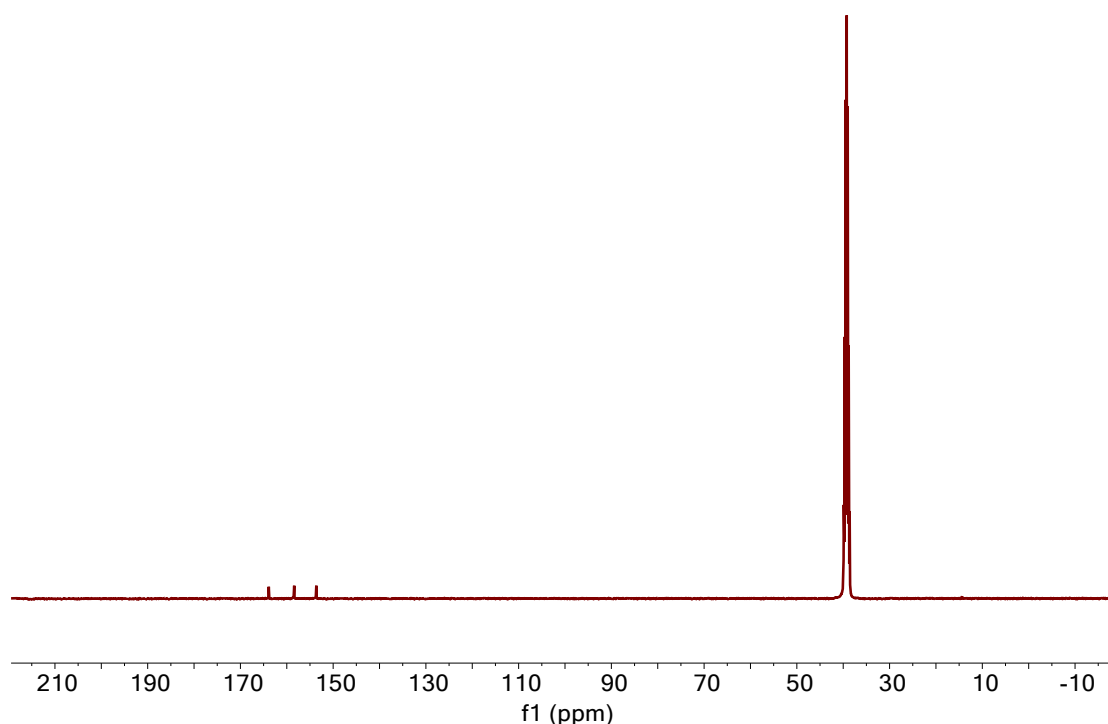
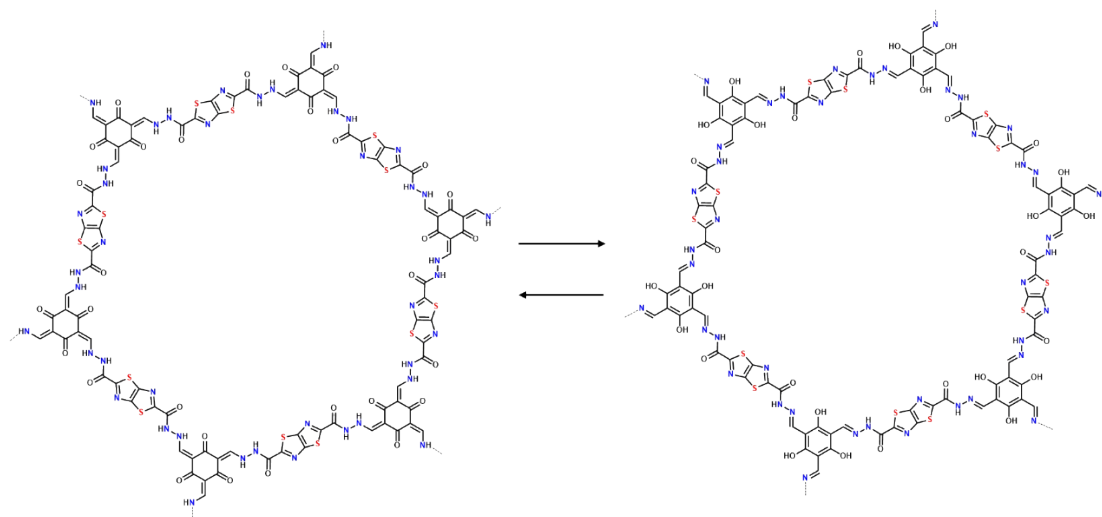


Fig. S2. ^{13}C NMR spectra of 2,5-thiazolo[5,4-*d*]thiazolidedicarboxylic hydrazide.

2.4 Synthesis of POP

In a typical process, Tz (11.6 mg, 0.045 mmol) and Tp (6.3 mg, 0.03 mmol) were charged in a 10 mL Schlenk tube with 1.50 mL of *o*-dichlorobenzene, 0.50 mL of dioxane, and 0.20 mL of 6 M acetic acid aqueous solution. The tube was flash-frozen at 77 K in a liquid-nitrogen bath and degassed with three freeze-pump-thaw cycles. After warming to room temperature, the mixture was ultrasonicated for 30 min and then heated at 120 °C for 72 h. The red-yellow solid was isolated by filtration, washed and solvent exchanged with DMF and CH_3OH . The resultants were dried under vacuum at 100 °C for 24 h to afford POP powders (13.7 mg, 84%).



Keto-enol tautomerism in POP.

2.5 Synthesis of POP-Fe

Typically, POP (30.0 mg) and $\text{Fe}(\text{NO}_3)_3 \cdot 9\text{H}_2\text{O}$ (80.8 mg) were dispersed in 20.0 mL methanol and ultrasonicated for 30 min, then the mixture was stirred for 12 h at 60 °C. A formed precipitate was extracted by centrifugation, rinsed with water three times, and vacuum-dried at 70 °C for 24 h.

2.6 Synthesis of POP-Ni

Typically, POP (30.0 mg) and $\text{Ni}(\text{CH}_3\text{COO})_2 \cdot 4\text{H}_2\text{O}$ (49.7 mg) were dispersed in 20.0 mL methanol and ultrasonicated for 30 min, then the mixture was stirred for 12 h at 60 °C. A formed precipitate was extracted by centrifugation, rinsed with water three times, and vacuum-dried at 70 °C for 24 h.

2.7 Synthesis of POP-Fe/Ni

Typically, POP (30.0 mg), $\text{Fe}(\text{NO}_3)_3 \cdot 9\text{H}_2\text{O}$ (80.8 mg), and $\text{Ni}(\text{CH}_3\text{COO})_2 \cdot 4\text{H}_2\text{O}$ (49.7 mg) were dispersed in 20.0 mL methanol and ultrasonicated for 30 min, then the mixture was stirred for 12 h at 60 °C. A formed precipitate was extracted by centrifugation, rinsed with water three times, and vacuum-dried at 70 °C for 24 h.

2.8 Synthesis of POP-Metal-900

The above POP and POP-M (Fe, Ni, Fe/Ni) powder was pyrolyzed at 900 °C under N₂ ambient for 3 h. The obtained carbonized material was washed with dilute hydrochloric, water, and vacuum-dried at 100 °C for 24 h to afford POP-M (Fe, Ni, Fe/Ni)-900.

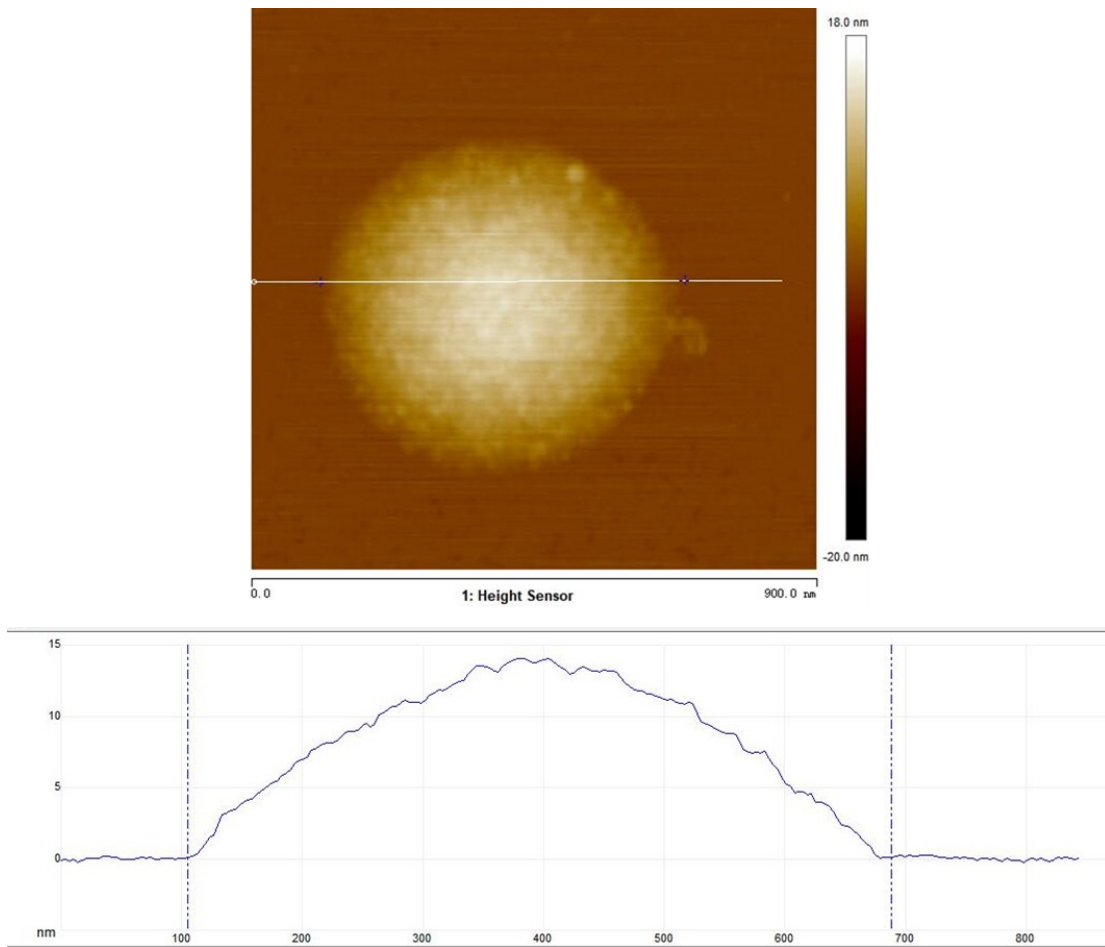


Fig. S3. Atomic force microscope imaging of POP.

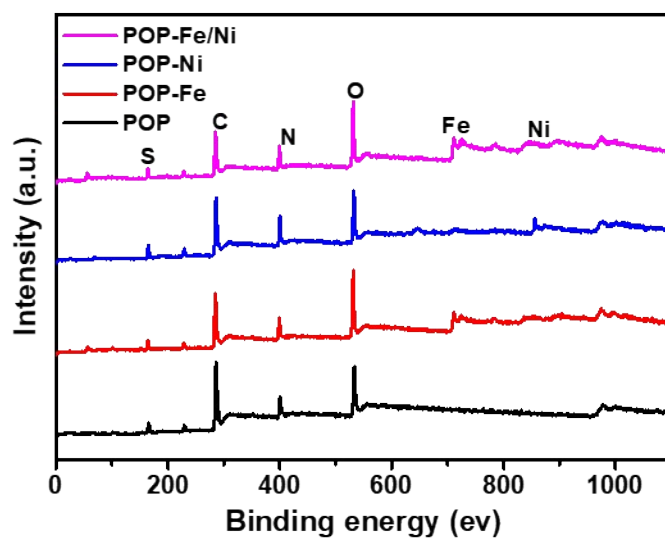


Fig. S4. XPS spectra of POP, POP-Fe, POP-Ni, and POP-Fe/Ni.

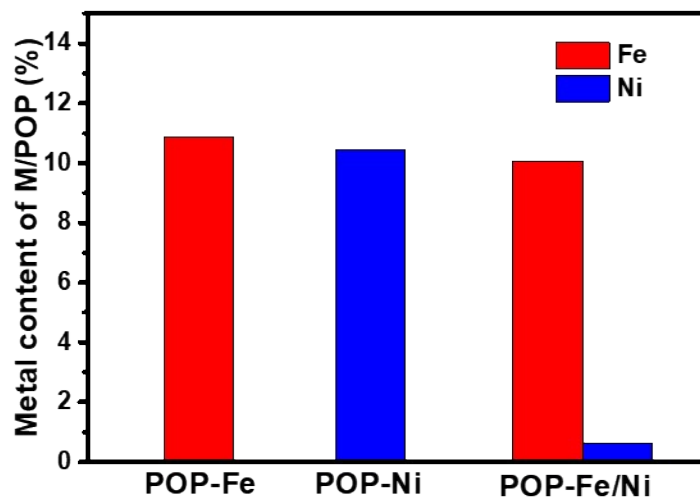


Fig. S5. Metal content loading in POP.

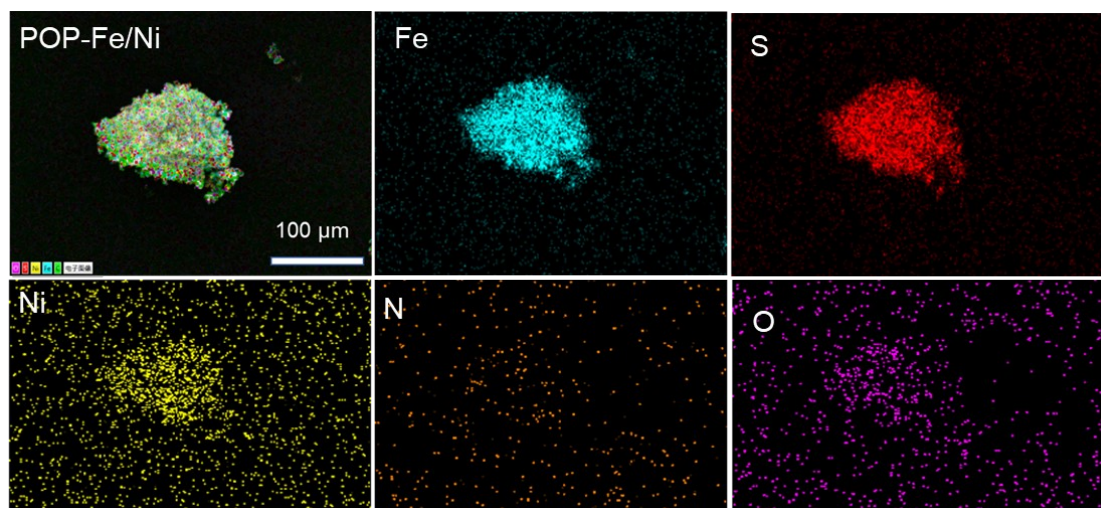


Fig. S6. Elemental mapping images of POP-Fe/Ni. Scale bar = 100 μm .

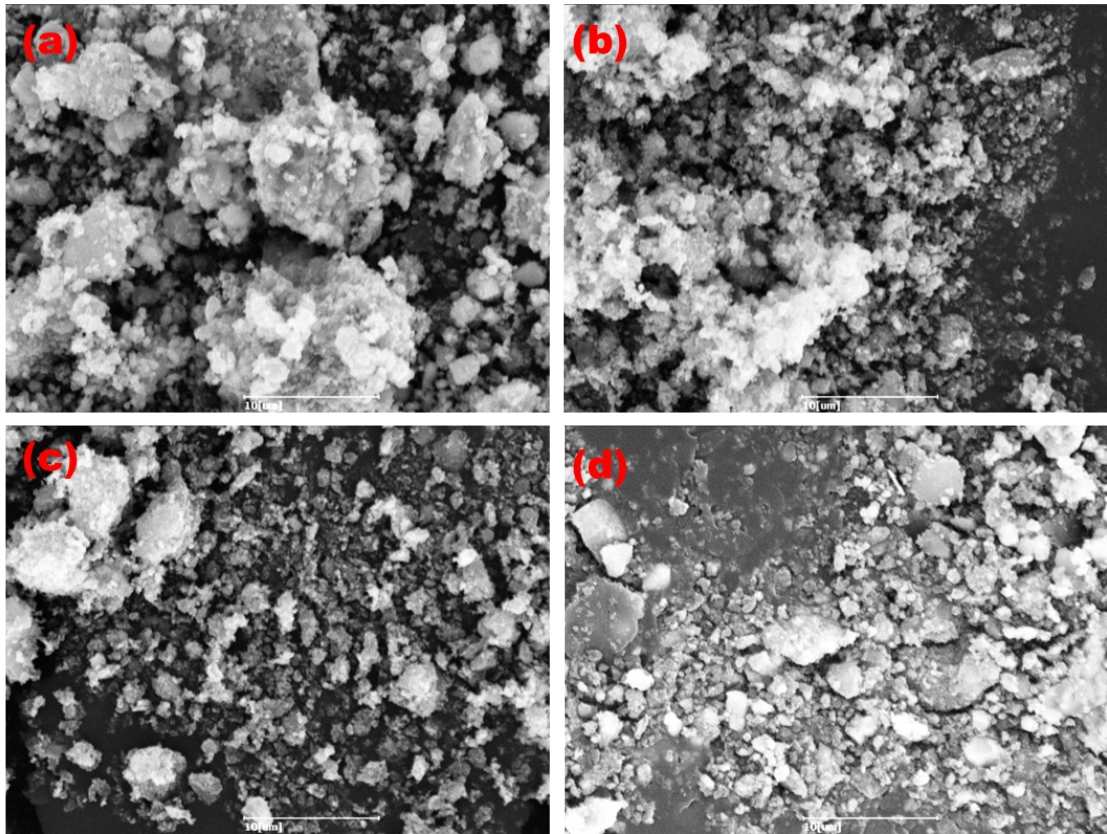


Fig. S7. SEM images of (a) POP-900, (b) POP-Fe-900, (c) POP-Ni-900, (d) POP-Fe/Ni-900.
Scale bar = 10 μm .

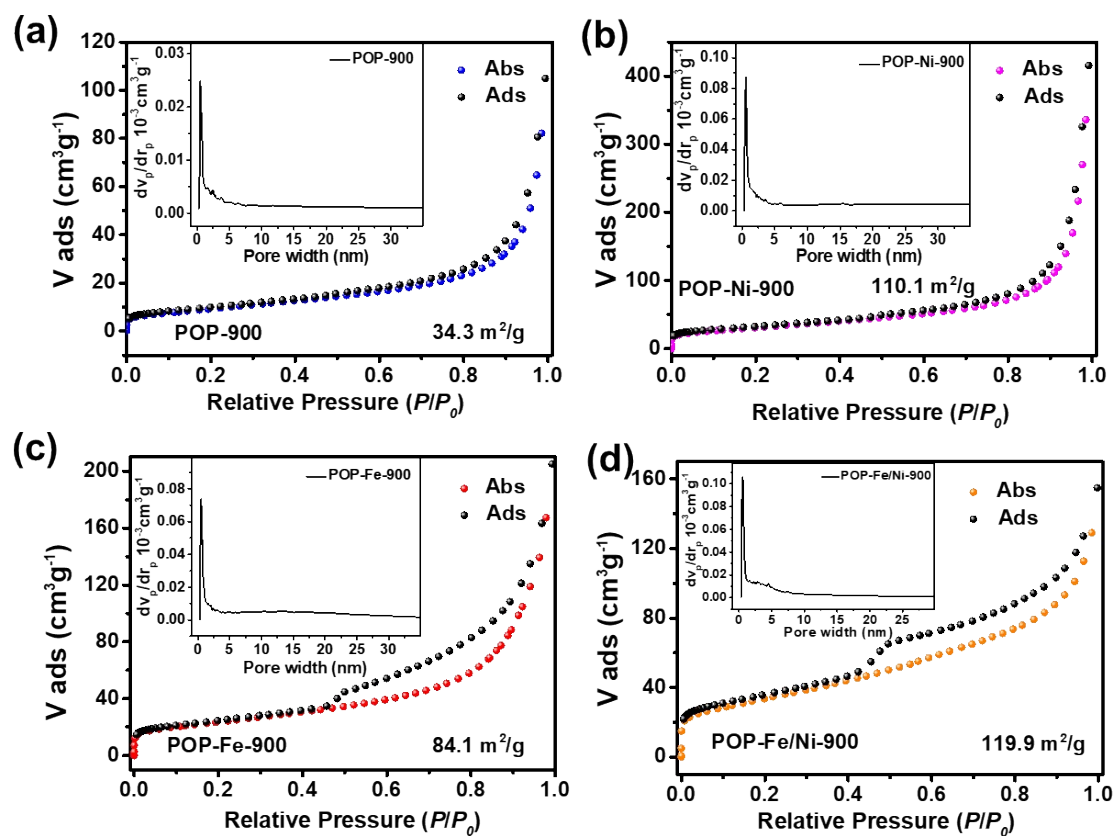


Fig. S8. N_2 sorption isotherms of the POP-900, POP-Ni-900, POP-Fe-900, and POP-Fe/Ni-900 at 77 K and corresponding pore size distribution.

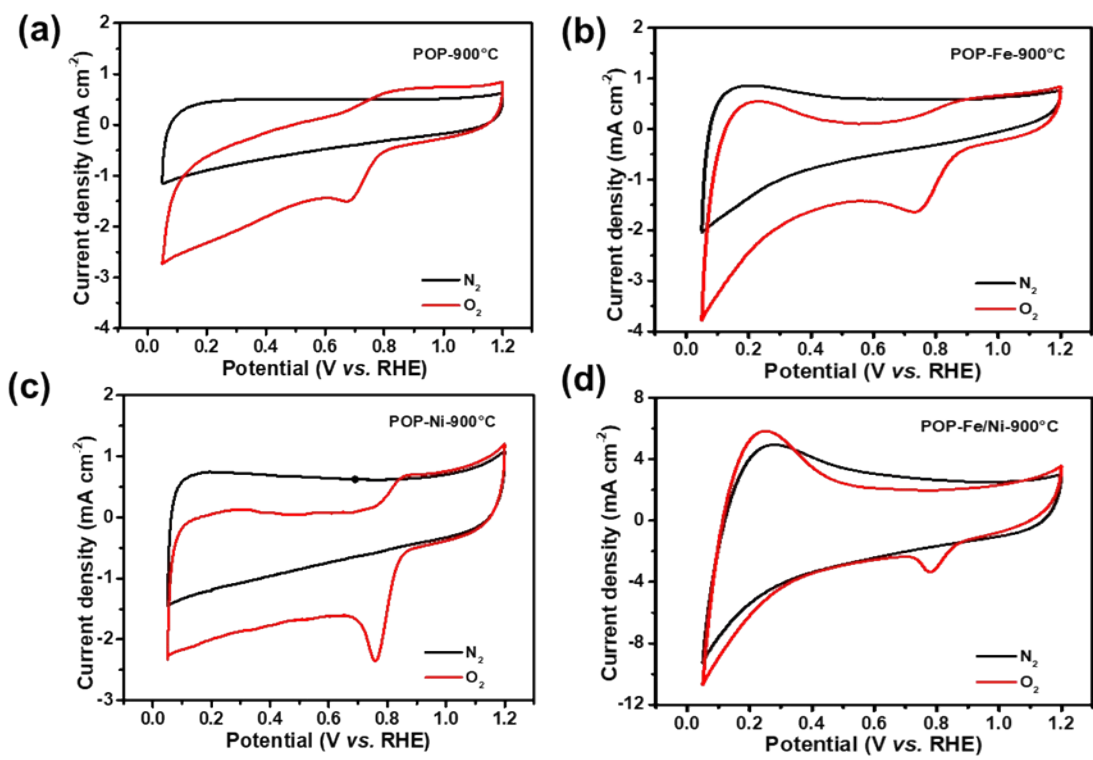


Fig. S9. CV curves of POP-Fe/Ni-900 in O₂/N₂ saturated 0.1 M KOH.

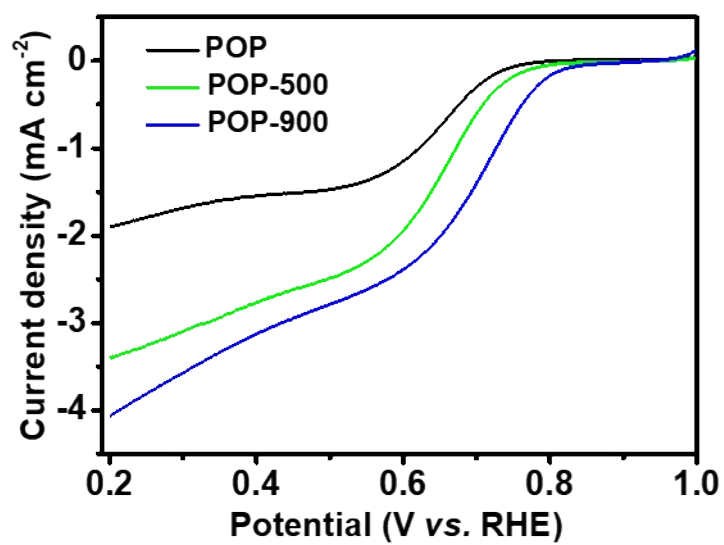


Fig. S10. The LSV curves of POP (without pyrolysis), POP-500, and POP-900 for ORR process in 0.1 M KOH at 1600 rpm.

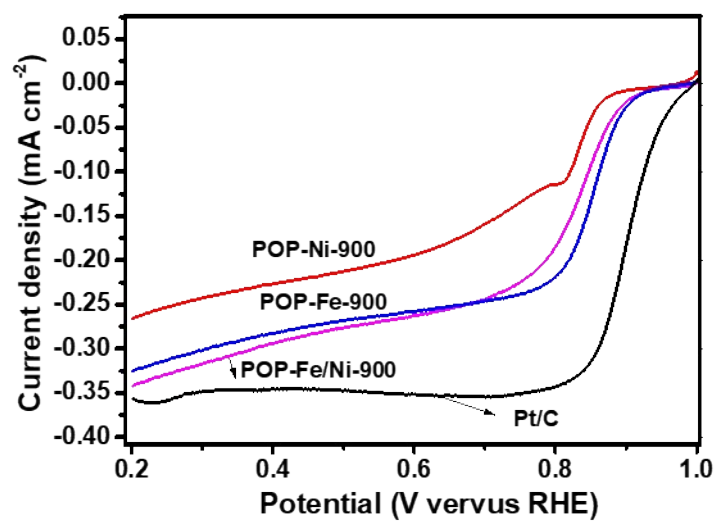


Fig. S11. The LSV curves of POP-derived carbon materials for ORR process in 6 M KOH at 1600 rpm.

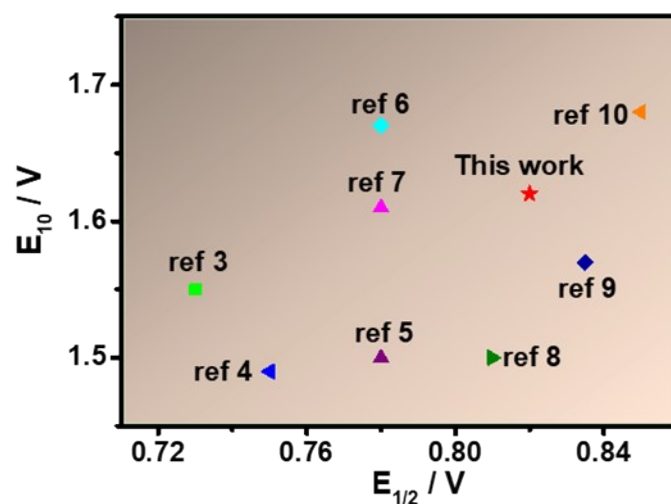


Fig. S12. Electrocatalytic activity of POP-Fe/Ni-900 and other recently reported bifunctional catalysts.³⁻¹¹ The X-axis represents ORR activity at the half-wave potential ($E_{1/2}$). The Y-axis represents OER activity when the current density is 10 mA/cm² (E_{10}).

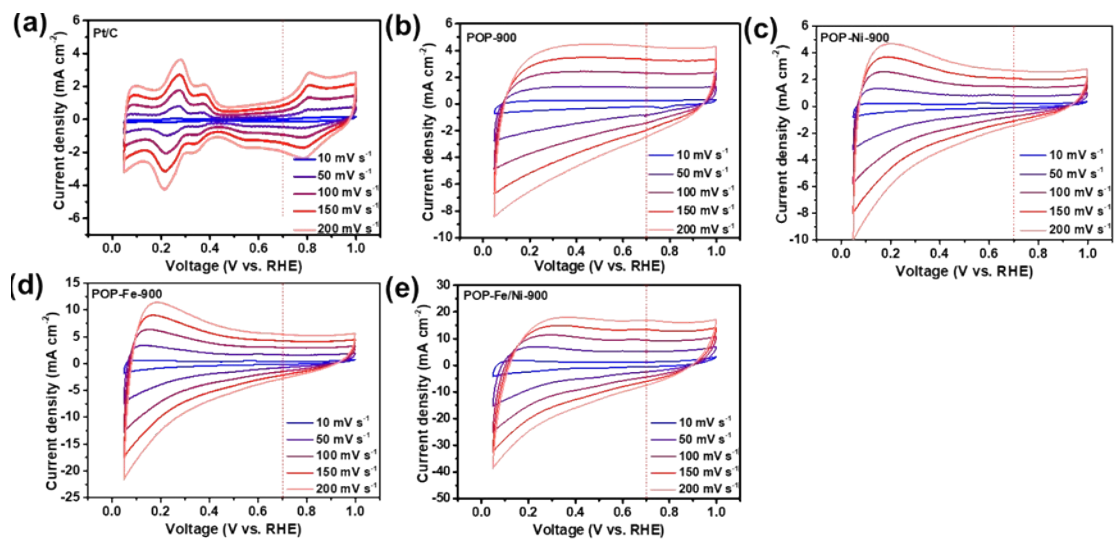


Fig. S13. CV curves for (a) Pt/C, (b) POP-900, (c) POP-Ni-900, (d) POP-Fe-900, and (e) POP-Fe/Ni-900 at various scan rates.

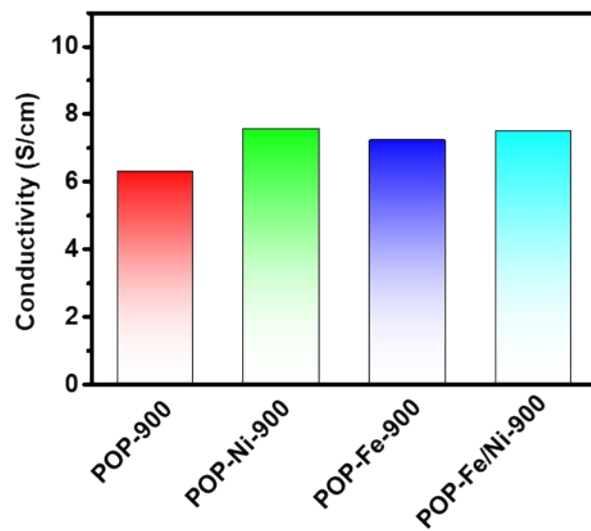


Fig. S14. Electrical conductivity of POP-900, POP-Ni-900, POP-Fe-900, and POP-Fe/Ni-900 at 25°C.

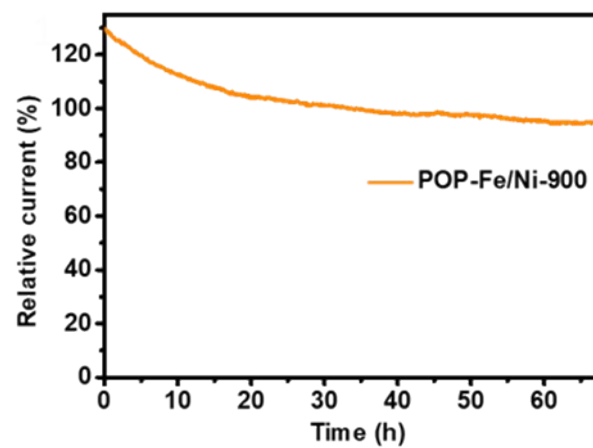


Fig. S15. The chronoamperometric curves of POP-Fe/Ni-900 at + 0.50 V for 67 h.

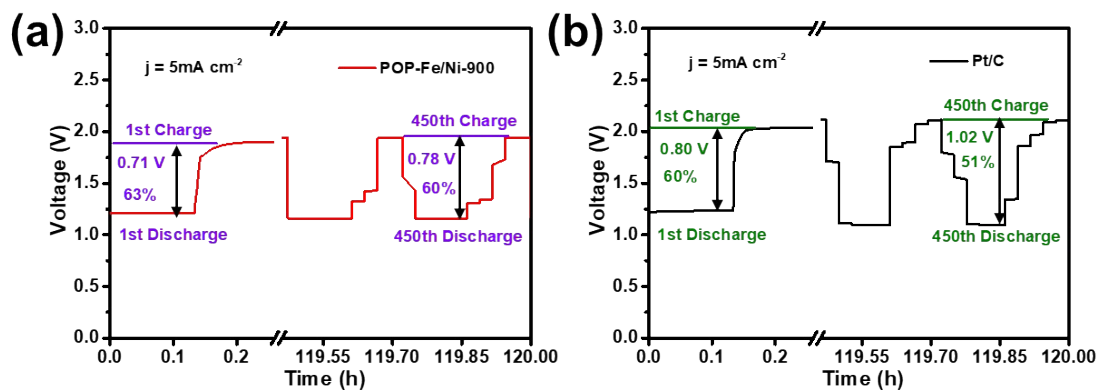


Fig. S16. The discharge and charge voltage profiles of ZABs with (a, b) POP-Fe/Ni-900 catalyst and conventional Pt/C catalyst at a current density of 5 mA cm^{-2} at room temperature, respectively.

References

1. John Raven Johnson, Don H. Rotenberg, and Roger Ketcham. *J. Am. Chem. Soc.*, 1970, **92**, 4046-4050.
2. R. F. P. Clementino, A. B. de Souza Santos, O. J. B. J. Marques, D. R. Ratkovski, C. C. Gatto, I. Malvestiti, F. L. de Araujo Machado and E. H. L. Falcão, *J. Solid. State. Chem.*, 2018, **268**, 94-101.
3. Q. Wang, L. Shang, R. Shi, X. Zhang, G. I. N. Waterhouse, L.-Z. Wu, C.-H. Tung and T. Zhang, *Nano Energy*, 2017, **40**, 382-389.
4. L. Diao, T. Yang, B. Chen, B. Zhang, N. Zhao, C. Shi, E. Liu, L. Ma and C. He, *J. Mater. Chem. A*, 2019, **7**, 21232-21243.
5. D. Ren, J. Ying, M. Xiao, Y. P. Deng, J. Ou, J. Zhu, G. Liu, Y. Pei, S. Li, A. M. Jauhar, H. Jin, S. Wang, D. Su, A. Yu and Z. Chen, *Adv. Funct. Mater.*, 2020, **30**, 1908167.
6. Y. S. Wei, M. Zhang, M. Kitta, Z. Liu, S. Horike and Q. Xu, *J. Am. Chem. Soc.*, 2019, **141**, 7906-7916.
7. Y. Guo, S. Yao, L. Gao, A. Chen, M. Jiao, H. Cui and Z. Zhou, *J. Mater. Chem. A*, 2020, **8**, 4386-4395.
8. Y. W. Li, W. J. Zhang, J. Li, H. Y. Ma, H. M. Du, D. C. Li, S. N. Wang, J. S. Zhao, J. M. Dou and L. Xu, *ACS Appl. Mater. Interfaces.*, 2020, **12**, 44710-44719.
9. J. Tan, T. Thomas, J. Liu, L. Yang, L. Pan, R. Cao, H. Shen, J. Wang, J. Liu and M. Yang, *Chem. Eng. J.*, 2020, **395**, 125151
10. X. Zhang, P. Yu, G. Xing, Y. Xie, X. Zhang, G. Zhang, F. Sun and L. Wang, *Small*, 2022, **18**, e2205228.
11. W. Zhu, H. Liu, R. Yue, Y. Pei, J. Zhang, X. Liu, R. Li, Y. Yin and M. D. Guiver, *Small*, 2022, **18**, e2202660.